NeuroImage **11,** 49–57 (2000)
doi:10.1006/nimg.1999.0515, available online at http://www.idealibrary.com on IDEAL®

Characterization and Correction of Interpolation Effects in the Realignment of fMRI Time Series

S. Grootoonk, C. Hutton, J. Ashburner, A. M. Howseman, O. Josephs, G. Rees, K. J. Friston, and R. Turner

Wellcome Department of Cognitive Neurology, Institute of Neurology, University College London, London WC1N 3BG, United Kingdom

Received March 23, 1999

Subject motion in functional magnetic resonance imaging (fMRI) studies can be accurately estimated using realignment algorithms. However, residual changes in signal intensity arising from motion have been identified in the data even after realignment of the image time series. The nature of these artifacts is characterized using simulated displacements of an fMRI image and is attributed to interpolation errors introduced by the resampling inherent within realignment. A correction scheme that uses a periodic function of the estimated displacements to remove interpolation errors from the image time series on a voxel-by-voxel basis is proposed. The artifacts are investigated using a brain phantom to avoid physiological confounds. Small- and large-scale systematic displacements show that the artifacts have the same form as revealed by the simulated displacements. A randomly displaced phantom and a human subject are used to demonstrate that interpolation errors are minimized using the correction.

Key Words: **fMRI; interpolation; motion artifacts.**

INTRODUCTION

It has been accepted for some time that changes in signal intensity in functional magnetic resonance imaging (fMRI) time series can arise from head motion. In the analysis of functional activation studies, such changes in the fMRI signal can be confused with signal changes due to brain activity, when the movement is correlated with the task (Hajnal *et al.,* 1994). If there is no correlation between the task and the movement, it is unlikely that artifactual activations will be attributed to brain activity, although the detection of true activations may be impaired due to the increase in error variance. Realignment of three-dimensional images in a time series can provide accurate registration, but alone is not sufficient to correct for all signal changes due to motion. It has been shown that signal changes can arise from a change of the position of the object in the scanner and from movement of the object in previous scans (Friston *et al.,* 1996). The latter has come to be known as the spin history effect and occurs when excited spins in the acquisition volume do not have time to return to equilibrium before the next excitation pulse occurs, that is, when the repetition time, TR, is comparable to the relaxation time, T1. The practical considerations of correcting for these effects have recently been explored (Robson *et al.,* 1997). Here we do not consider changes in the fMRI signal due to the spin history effect. In the data presented the TR is greater than 4 s, which is long enough for this effect to be negligible. We are concerned with the form and origin of the components of the fMRI signal that are a simple function of the position of the object in the scanner. We consider displacements in the in-plane (x and y directions) as well as the z direction. In this context it is worth noting that it is important to use small slice gaps and square slice profiles to ensure data sufficiency (Noll *et al.,* 1997).

Image realignment may be considered as a two-part process. First, each scan in the time series is coregistered to a target, which is usually the first scan in the time series. In coregistration, a series of six-parameter, rigid-body transformations (translations in the x, y, and z directions and rotations about the x, y, and z axes) is estimated by minimizing a function of the difference between the object and the target images. A least-squares solution is found, giving a six-parameter estimation for the movements associated with each scan (Woods *et al.,* 1992; Friston *et al.,* 1995). Realignment algorithms based on this approach can achieve an accuracy in the range 50 μm or better (Jiang *et al.,* 1995; Frouin *et al.,* 1997).

The second part of the realignment process involves resampling each image according to the spatial transformation estimated in the first stage. The intensity of each voxel in the transformed image must be determined from the intensities in the original image. In order to realign images with subvoxel accuracy, the spatial transformations will involve fractions of a voxel. It is therefore necessary to resample the image at positions between the centers of voxels. This requires

1053-8119/00 $35.00

an interpolation scheme to estimate the intensity of a voxel, based on the intensity of its neighbors. A rudimentary approach is to take the value of the closest neighboring voxel. This is referred to as nearest neighbor resampling, which does not correct for intensities at subvoxel displacements. A better approach is trilinear interpolation, which computes the intensity of transformed voxels by a position-dependent linear weighted-average of eight neighboring voxels. This accounts for subvoxel displacements but also removes some high spatial frequency information from the image. Trilinear interpolation is simple to implement and has a relatively high computational speed; however, it can still introduce sampling errors (Ostuni *et al.,* 1997).

The ideal scheme for transforming band-limited MR images without introducing artifacts is to perform the translations and rotations in Fourier space. This approach is referred to as Fourier interpolation and has been implemented in two dimensions (Eddy *et al.,* 1996). The image–space method that gives the closest results to Fourier interpolation is a full sinc interpolation using every voxel in the image to calculate the new value at a single voxel (Jain, 1989). The slowest procedure in fMRI data analysis is the accurate realignment of the image time series. Because of the computational burden of performing a full sinc interpolation, in practice it is necessary to limit the extent of the sinc function (Hajnal *et al.,* 1995). The truncated sinc function is commonly implemented using an 11-voxel Hanning-windowed sinc function. For a data matrix of 48 64×64-voxel slices, realignment using an 11-voxel sinc kernel proceeds at a rate of about 1 min per volume on a Sparc 20 Sun workstation. This increases 200-fold if a 64-voxel kernel is employed.

This paper investigates the form of intensity artifacts introduced by this nonideal interpolation scheme and explores the relationship with motion-correlated signal changes. In the context of current high-resolution fMRI studies, it is important to investigate displacements of the order of several voxels. Several experiments are presented. A simulation is used to directly address the question of interpolation artifacts and to characterize their form. A correction algorithm for interpolation errors, with computational times compatible with routine fMRI studies, is derived from these results. Signal changes due to motion are investigated and characterized with a brain phantom to avoid physiological signal changes. The effects of motion in a human fMRI activation study are also investigated. The correction for interpolation artifacts is applied to the phantom data and the fMRI time series and its impact assessed.

MATERIALS AND METHODS

All fMRI studies were performed on a Siemens Magnetom Vision scanner operating at 2 T, using either a 64-slice 2D gradient echo planar (EPI) sequence (image array of $64 \times 64 \times 64$ voxels) or a single-slice FLASH sequence (image array 64×64). Both sequences had in-plane resolution of 3 mm, slice thickness of 1.8 mm, and slice separation of 1.2 mm. Simulated displacements of image data were performed in Matlab (The Math Works, Inc.). All realignments were performed using the standard realignment algorithm in SPM96 (Friston *et al.,* 1995), which resamples the realigned data using an 11-voxel Hanning-windowed sinc function interpolation kernel in three dimensions.

The effect of object movement was investigated using a Hoffman brain phantom (Hoffman *et al.,* 1990). This phantom consists of a stack of Perspex slices cut to an anatomical MRI template, contained in an outer, cylindrical, Perspex shell, resulting in a three-dimensional structure with two compartments. One compartment, the Perspex, simulates the central brain structures and cerebrospinal fluid, and the other compartment, the fillable cavity, structurally simulates the features of the human cortex. This phantom was designed to be filled with a radioactive solution and imaged using emission tomography to mimic the distribution of a tracer of metabolism in the human brain. For MR imaging, the cavity was filled with tap water. Representative EPI images of the brain phantom are shown in Fig. 1 (top).

The effects of subject motion on fMRI data were characterized in a human study using an auditory stimulus. The volunteer was presented with binaural spoken words (one word per second). The subject's head was cushioned inside the Siemens proprietary head rf coil assembly, and two adjustable pads exerted light pressure to either side of the head. This is the standard method of immobilization in our laboratory. Representative EPI images of the subject are shown in Fig. 1 (bottom).

EXPERIMENTS

Simulated Movements

Characterization of Interpolation Artifacts

A simulated image time series was generated using a single slice (64×64 voxels) from an EPI image volume of a subject scanned at rest. Each point in the time series was created by sequentially translating the slice by a subvoxel displacement of 0.04 mm, spanning $\pm$ 1 voxel (generating 150 slices with a total displacement of 6 mm). The translated slice was generated at each displacement by resampling the original slice using a 64-voxel Hanning-windowed sinc function. This interpolation gave negligible error when applied repeatedly, showing its close equivalence to Fourier interpolation. The translated slices thus obtained were realigned and resampled using the standard SPM96 realignment

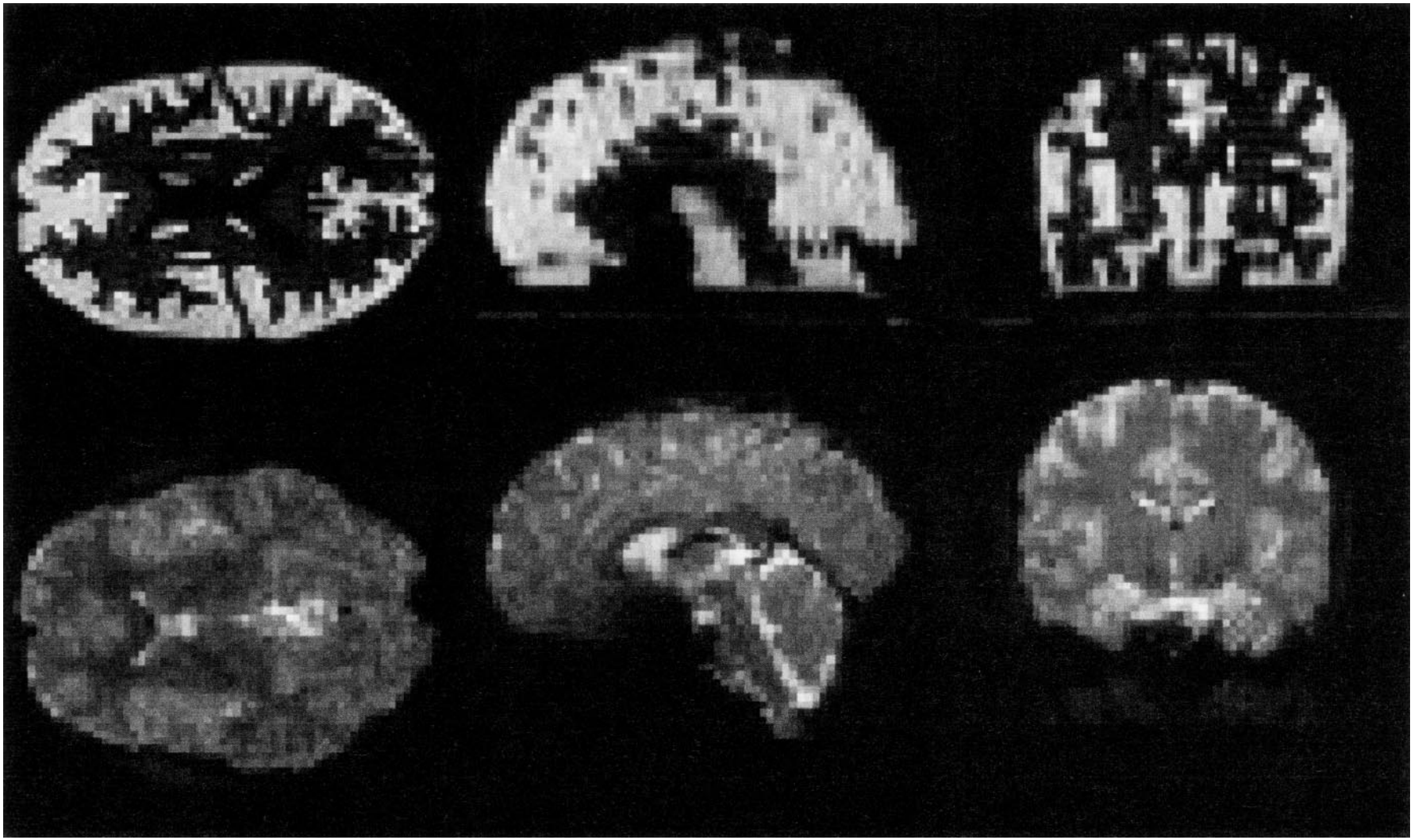

FIG. 1. Transaxial, sagittal, and coronal slices through a single fMRI volume of the brain phantom (top) and the human subject (bottom).

procedure, which employs an 11-voxel Hanning-windowed sinc function for reasons of computational speed. Principal component analysis (PCA) was performed on the resulting realigned time series to characterize the functional form of the time dependence of the intensity variations (Fig. 2). The periodic functions in Fig. 2 describe how the greatest amounts of variance–covariance in the data vary with displacement over 2 voxels. There are two main components of different magnitudes, which vary sinusoidally with a common period of one voxel. The major form of errors is therefore periodic and can be described by two functions,

$$\begin{matrix} \sin 2\pi t \\ \cos 2\pi t, \end{matrix} \quad (1)$$

where t is the displacement in voxels.

Correction for Interpolation Artifacts

It has previously been reported that residual movement-related artifacts in realigned images are reduced by covarying out (i.e., regressing) signal correlated with functions of the motion estimates (Friston *et al.,* 1996). These functions comprised a first- and second-order term to approximate linear and nonlinear motion-dependent effects. In our simulations, we have identified that these artifacts can be largely explained by interpolation errors. When the displacements are of the order of one voxel or more, these errors are best described by two periodic functions. We therefore propose replacing the linear and nonlinear functions of movement above with periodic functions of movement to remove residual signal changes after realignment.

For each voxel in the two-dimensional image, a matrix $\mathbf{M}$ is generated as a function of the displacements in x and y at each of J time points.

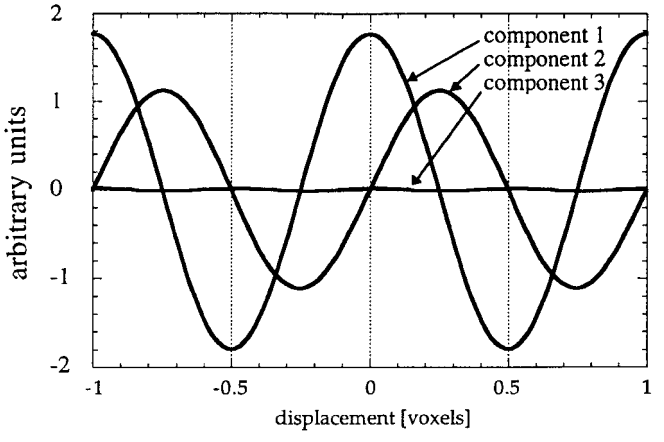

FIG. 2. PCA of the realigned images from the simulated time series as a function of displacement. The first and second principal components of realigned images show how the variance–covariance in the time series vary periodically with displacement.

$$\mathbf{M} = \begin{bmatrix} \sin(2\pi x_1) & \cos(2\pi x_1) & \sin(2\pi y_1) & \cos(2\pi y_1) & 1 \\ \sin(2\pi x_2) & \cos(2\pi x_2) & \sin(2\pi y_2) & \cos(2\pi y_2) & 1 \\ \vdots & \vdots & \vdots & \vdots & \vdots \\ \sin(2\pi x_J) & \cos(2\pi x_J) & \sin(2\pi y_J) & \cos(2\pi y_J) & 1 \end{bmatrix} \quad (2)$$

We model movement effects for each voxel time course b linearly as

$$b = \mathbf{M}p + r, \quad (3)$$

where r represents the residuals. Coefficients p are determined that best fit the columns of $\mathbf{M}$ to the voxel time course b in a least-squares sense (i.e., minimize r^2):

$$p = (\mathbf{M}^{\mathrm{T}}\mathbf{M})^{-1}\mathbf{M}^{\mathrm{T}}b. \quad (4)$$

Any component of the signal in b that is correlated with the first four columns of $\mathbf{M}$ is then removed from b:

$$b^* = b - \begin{bmatrix} p_1 \\ p_2 \\ p_3 \\ p_4 \\ 0 \end{bmatrix} \mathbf{M}. \quad (5)$$

This correction involves creating a separate adjustment matrix $\mathbf{M}$ for each voxel related to the estimated displacements of that voxel over the whole time series. There is a natural extension of the correction to the three-dimensional case, and the use of voxel-specific correction matrices implicitly deals with rotations.

Displacement of Brain Phantom

The brain phantom was moved relative to the imaging field of view both in a systematic manner, by shifting the field of view of the scanner, and also randomly by manually applying small displacements to the phantom within the scanner field of view. Images were collected, realigned, and resampled and analyzed both with and without the correction for the interpolation artifacts described above.

Systematic Displacements

Small- and large-scale displacements in the slice-select or z direction were achieved by moving the field of view in 0.1-mm steps over two slices (6 mm total displacement) and in 0.5-mm steps covering five slices (15 mm total displacement). A single EPI volume was acquired at each displacement for both small- and large-scale movements. The same displacements were investigated for within-plane motion by moving the

field of view in the readout or *x* direction. In this case, single-slice FLASH data were acquired.

The estimates of translation in the *x, y,* and *z* directions were plotted against scan number to illustrate the systematic, small-scale, movements over time (Fig. 3, top). Principal component analysis was performed on the realigned images (Fig. 3, middle). The effect of the correction for interpolation artifacts is demonstrated by representative voxel time courses (Fig. 3, bottom). The data in Fig. 3 illustrate small displacements in the *z* direction. The effects seen were also reproduced with small displacements in the *x* direction and large displacements in the *z* direction and in the *x* direction. Before correction, the intensity over the time courses varies sinusoidally with a period of one cycle per unit voxel displacement. This periodic compo-

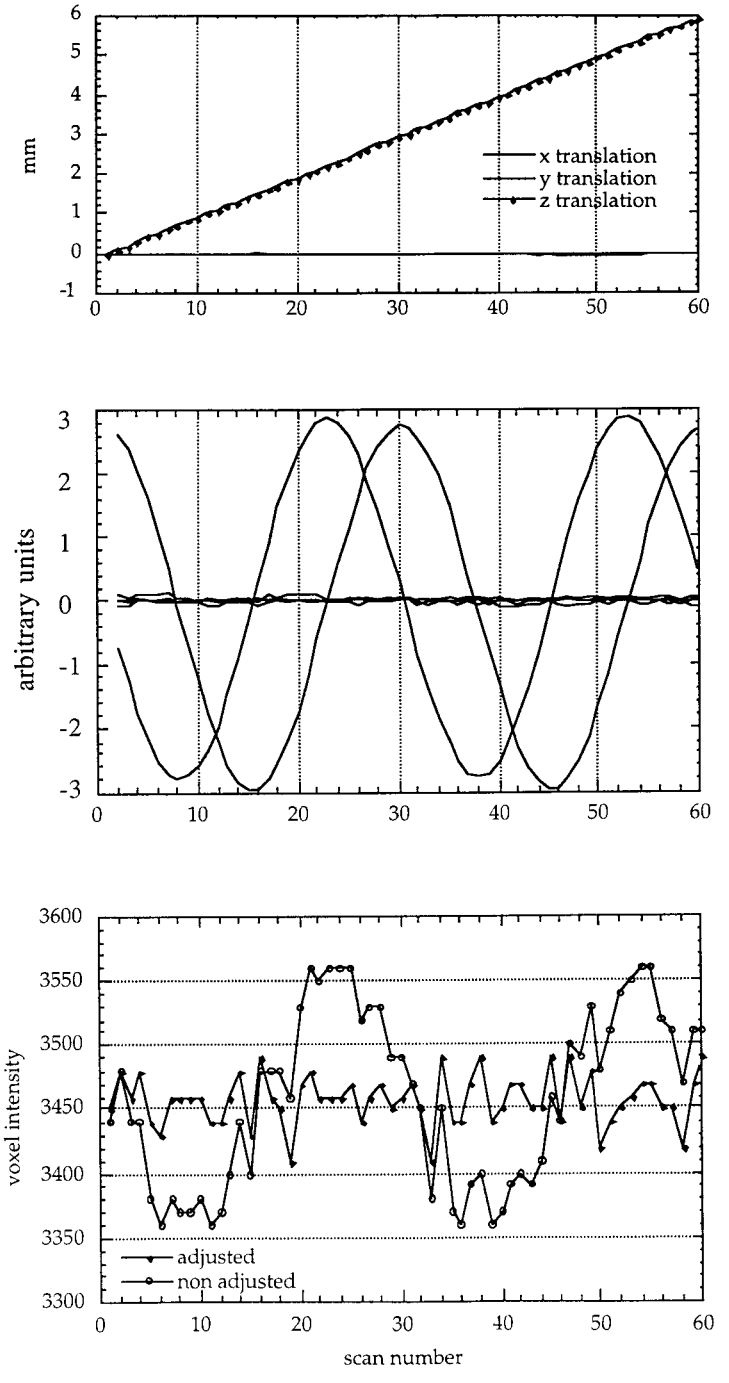

FIG. 3. Results of systematic displacements of the brain phantom. (Top) Estimated realignment parameters, (middle) PCA of realigned images, and (bottom) voxel time courses before and after adjustment plotted against scan number.

nent is seen to be attenuated strongly after applying the correction. The mean variance over the time series was calculated for small and large displacements in the *x* and *z* directions, before realignment, and after realignment, both before and after the correction for interpolation effects. The results demonstrate a factor of 40 reduction in variance after realignment and a further factor of 10 reduction in variance following the correction.

Random, Manual Displacements

To mimic movement of a human subject in the field of view, the brain phantom was moved manually within the scanner by discrete displacements. In order to control these displacements and avoid intrascan motion, the phantom was moved rapidly in the intervals between scans. One movement was made every fifth scan. The estimates of translation in the *x, y,* and *z* directions were plotted against scan number to illustrate the applied movement over time (Fig. 4, top). The time course of a representative voxel from the realigned time series was plotted to demonstrate the effect of the adjustment (Fig. 4, bottom). The time course from this voxel shows a reduction in signal change from a maximum of 10% to around 2% after applying the adjustment. Signal changes that appear to be highly correlated with motion are removed. Variance images over the time series were also calculated and a representative slice is shown in Fig. 5. Before the correction, the highest variance can be seen at the boundaries between compartments and edges of the object. After the correction, a factor of 10 reduction in variance was observed over the whole object.

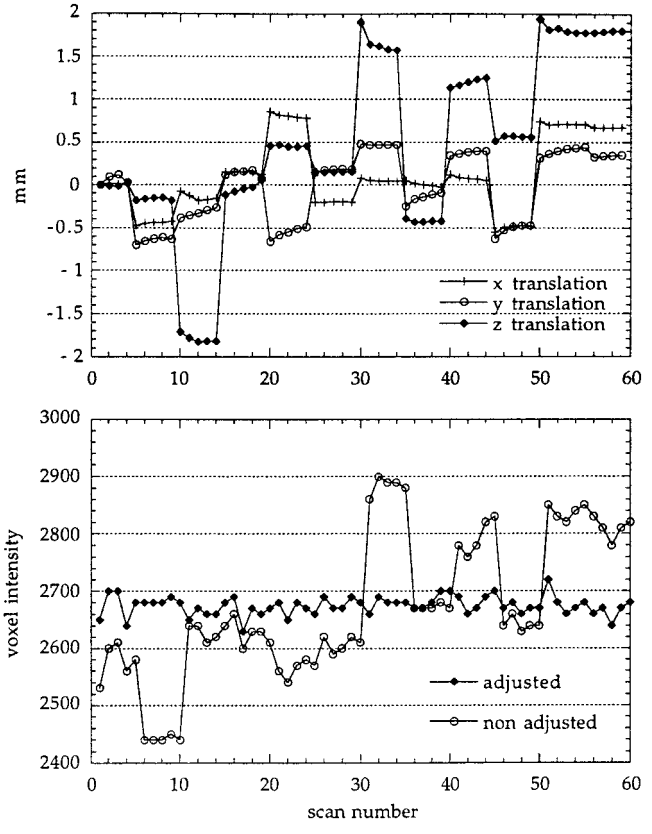

FIG. 4. Results of random, manual displacements of brain phantom. (Top) Estimated realignment parameters and (bottom) voxel time courses before and after adjustment.

Study of Movement in a Human Subject

The human study comprised 30-s blocks of an auditory stimulus alternated with 30-s rest blocks (6 scans per block, 10 blocks per condition, each scan of 5 s duration). A total of 120 brain image volumes were acquired over 10 min. The image time series of the human subject was realigned and resampled both with and without the adjustment for interpolation artifacts described above. The estimated translational movements in the *x, y,* and *z* directions were plotted against scan number to show how the subject moved throughout the experiment (Fig. 6, top). The subject moved gradually after the 60th scan, in the *z* direction. This gradual drift in position after a certain period of relative immobility is typical in our fMRI subjects. The maximum translation for this subject is less than half a voxel (1.5 mm).

The effect of the adjustment for interpolation is illustrated by showing the time course of selected voxels. The time courses of a representative voxel in the auditory cortex and a voxel in a frontal lobe gray-matter region are shown in Fig. 6, middle and bottom, respectively. Variance images over the time series were calculated to illustrate the effect of the correction for interpolation (Fig. 7). After applying the correction for interpolation errors, the variance was reduced by 10%, the effect being mostly visible around the edge of the brain and central structures. The correction had no effect on the *Z* score of the activated voxel, which had an value of 7.7.

DISCUSSION

We have emphasized the existence of residual intensity errors in fMRI time series even after realignment using accurate movement estimates. In particular we have demonstrated that if a nonideal interpolation scheme is used to resample realigned images, this can account for a major component of the residual artifacts.

Artifacts obtained with a truncated sinc interpolation scheme have been illustrated using simulated displacements of an image and reproduced experimentally by systematically moving a brain phantom relative to the field of view of the scanner. The form of these artifacts has been characterized by a simple function of the estimated displacements over the time series. The

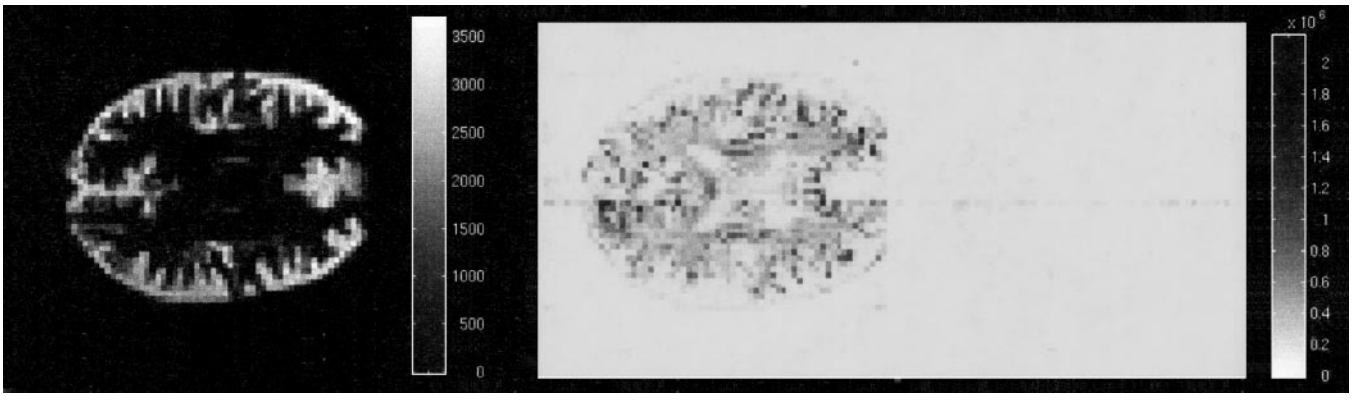

FIG. 5. Hoffman brain phantom: Mean image (left) and variance image for random displacements of the HBP before (center) and after (right) adjustment for interpolation artifacts. Note the relative importance of boundaries between areas of different signal intensity on the variance image before adjustment.

functions are periodic with a sine and a cosine component and a cycle of one voxel. This can be intuitively understood by recognizing that the resampling algorithm is exact for movements by integral numbers of voxels.

Our phantom experiments have shown that artifacts arise from movement in the *x*–*y* plane (readout or phase-encoding direction) as well as movement in the *z* direction (slice select). The function that characterizes these artifacts is the same in each case. For our experimental setup, image resolution, and voxel size, the function remains valid for displacements of up to 15 mm (five voxels).

These findings have allowed us to correct residual interpolation artifacts that are related to motion. The periodic function of the displacement that was determined using simulated data has been used to remove motion-correlated signal changes in the fMRI time series of *in vivo* data. The correction involves creating a separate adjustment matrix for each voxel in the image using voxel displacement parameters obtained by simple realignment. Within the SPM package, the adjustment has been implemented as an adjunct to the resampling step of the realignment process. There is only a minor computational overhead for each image resampled.

The results of the phantom experiments, in which we know there will be no signal changes due to physiological effects, clearly indicate the impact of the correction for interpolation artifacts. We have also explored the effect of the adjustment on a human study with typical small movements. The averaged variance over the

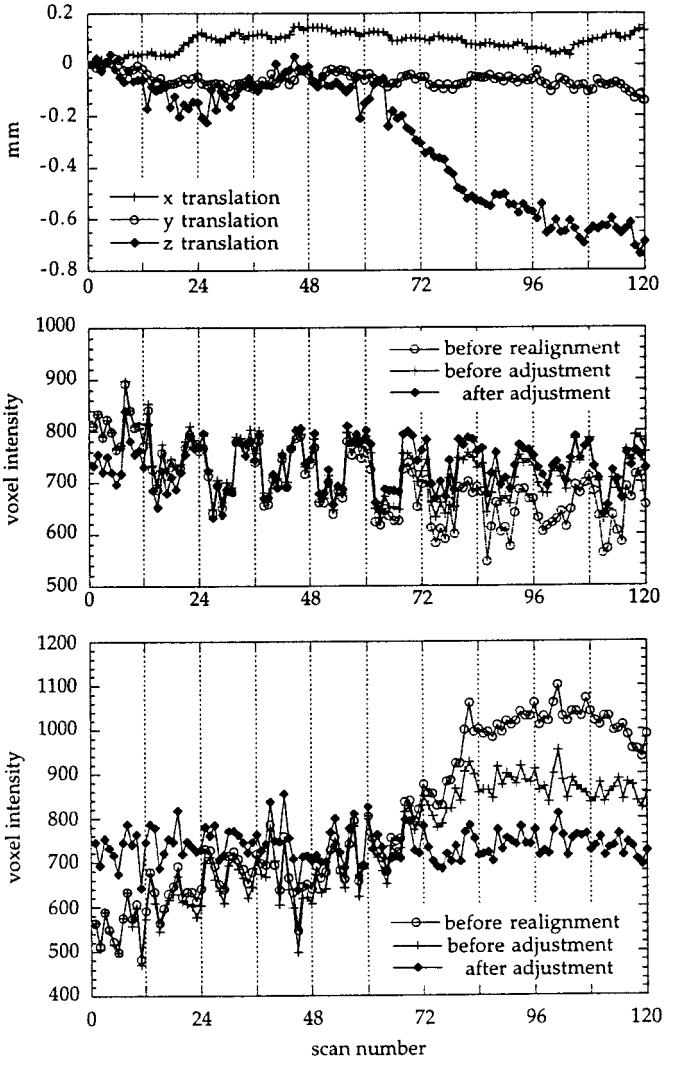

FIG. 6. Results of human auditory activation study. (Top) Estimated realignment parameters, (middle) voxel time course in an activated auditory region, and (bottom) a nonactivated region plotted against scan number. Time courses are shown for the data prior to image realignment and after realignment with and without adjustment.

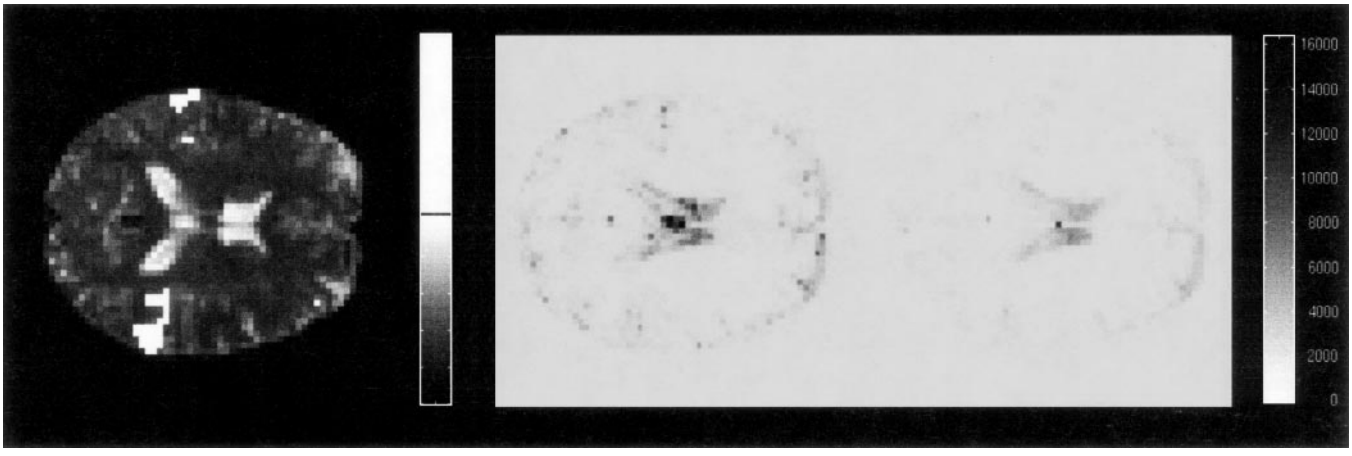

FIG. 7. Human auditory activation study. Mean image (left) and variance image before (center) and after (right) adjustment for interpolation artifacts.

volume in the time series is reduced by 10% and Fig. 7 shows that the main reductions occur in areas that are most affected by motion, e.g., around the edges of the volume, and internal tissue boundaries. Note that in these variance maps the variance associated with the auditory task has already been removed.

Task-correlated motion is an important issue which requires further investigation. If such motion is present, use of the algorithm described here inevitably results in reduced apparent activation. However, the protection from false positives may render this strategy desirable in some experimental contexts.

The adjustment reduces the degrees of freedom of the data set by the number of functions or columns used in the adjustment matrix. For the adjustment in three dimensions this number is 6, which is not of serious concern for fMRI experiments, in which it is not uncommon to acquire 100 or more image volumes. Often, fMRI experiments extend over tens of minutes. Low-frequency drifts have been observed in voxel time series and have been attributed to both scanner instability and physiological factors. High pass filtering of the data has been suggested as a correction for these effects (Holmes *et al.,* 1997). We find that artifacts due to subject motion are responsible for some low-frequency signal changes in our experimental data. These drifts were removed by the adjustment procedure presented here.

We have so far considered only interpolation artifacts which occur as a result of the movement between scans in the time series and used a postprocessing step to correct for them. Other motion-related artifacts can confound fMRI time series, such as intrascan subject motion, spin excitation history effects, and the interaction between motion and susceptibility artifacts (Birn *et al.,* 1997). These issues will need further investigation and may well be better addressed within the framework of data acquisition. Alternative approaches to fMRI data realignment can also be implemented as part of the data acquisition step, such as real-time motion correction (Lee *et al.,* 1996) and realignment in Fourier space (Eddy *et al.,* 1996).

Interpolation-based resampling errors have been demonstrated in realignment methods routinely used. Compared to the implementation of an ideal interpolation scheme, the correction for residual interpolation artifacts presented in this paper is a robust compromise which reduces the computational time to acceptable levels.

ACKNOWLEDGMENT

This work was funded by the Wellcome Trust.

REFERENCES

Birn, R. M., Jesmanowicz, A., Cox, R. W., and Shaker, R. 1997. Correction of dynamic B_z-field artifacts in EPI. In *Proc. ISMRM 5th Annual Meeting, Vancouver,* p. 1681.

Eddy, W. F., Fitzgerald, M., and Noll, D. C. 1996. Improved image registration by using Fourier interpolation. *Magn. Reson. Med.* **36:** 923–931.

Friston, K. J., Ashburner, J., Frith, C. D., Poline, J.-B., Heather, J. D., and Frackowiak, R. S. J. 1995. Spatial registration and normalization of images. *Hum. Brain Mapp.* **2:**165–189.

Friston, K. J., Williams, S., Howard, R., Frackowiak, R. S. J., and Turner, R. 1996. Movement-related effects in fMRI time-series. *Magn. Reson. Med.* **35:**346–355.

Frouin, V., Messegue, E., and Mangin, J.-F. 1997. Assessment of two fMRI motion correction algorithms. *Hum. Brain Mapp.* **5**:S458.

Hajnal, J. V., Mayers, R., Oatridge, A., Schwieso, J. E., Young, I. R., and Bydder, G. M. 1994. Artifacts due to stimulus correlated motion in functional imaging of the brain. *Magn. Reson. Med.* **31:** 289–291.

Hajnal, J. V., Saeed, N., Soar, E. J., Oatridge, A., Young, I. R., and Bydder, G. M. 1995. A registration and interpolation procedure for

subvoxel matching of serially acquired MR images. *J. Comput. Assist. Tomogr.* **19:**289–296.

Hoffman, E. J., Cutler, P. D., Digby, W. M., and Mazziotta, J. C. 1990. 3-D phantom to simulate cerebral blood flow and metabolic images for PET. *IEEE Trans. Nucl. Sci.* **37:**616–620.

Holmes, A. P., Josephs, O., Buchel, C., and Friston, K. J. 1997. Statistical modelling of low-frequency confounds in fMRI. *Hum. Brain Mapp.* **3:**S480.

Jain, A. K. 1989. *Fundamentals of Digital Image Processing.* Prentice Hall, New York.

Jiang, A. P., Kennedy, D. N., Baker, J. R., Weisskoff, R. M., Tootell, R. B. H., Woods, R. P., Benson, R. R., Kwong, K. K., Brady, T. J., Rosen, B. R., and Belliveau, J. W. 1995. Motion detection and correction in functional MR imaging. *Hum. Brain Mapp.* **3:**224–235.

Lee, C. C., Jack, C. R., Grimm, R. C., Rossman, P. J., Felmlee, J. P., Ehman, R. L., and Riederer, S. J. 1996. Real-time adaptive motion correction in functional MRI. *Magn. Reson. Med.* **36:**436–444.

Noll, D. C., Boada, F. E., and Eddy, W. F. 1997. A spectral approach to analyzing slice selection in planar imaging: Optimization for through-plane interpolation. *Magn. Reson. Med.* **38:**151–160.

Ostuni, J. L., Santha, A. K. S., Mattay, V. S., Weinberger, D. R., Levin, R. L., and Frank, J. A. 1997. Analysis of interpolation effects in the reslicing of functional MR images. *J. Comput. Assist. Tomogr.* **21:** 803–810.

Robson, M. D., Gatenby, J. C., Anderson, A. W., and Gore, J. C. 1997. Practical considerations when correcting for movement-related effects present in fMRI time-series. In *Proc. ISMRM 5th Annual Meeting, Vancouver,* p. 1681.

Woods, R. P., Cherry, S. R., and Mazziotta, J. C. 1992. Rapid automated algorithm for aligning and reslicing PET images. *J. Comput. Assist. Tomogr.* **16:**620–633.